

# Thermal Diffusivity and Conductivity of Crystalline Polymers

C. L. CHOY, E. L. ONG, and F. C. CHEN, *Department of Physics, The Chinese University of Hong Kong, Hong Kong*

## Synopsis

The thermal diffusivity and conductivity of the isotropic and drawn samples of five semicrystalline polymers—nylon 6, poly(ethylene terephthalate), poly(butylene terephthalate), polybutene-1, and poly(4-methylpentene-1)—were measured by the flash method over the temperature range 100–350 K. The temperature dependence of the thermal diffusivity was found to follow a simple phenomenological pattern, while a more detailed understanding of the temperature dependence and the effect of orientation on thermal conductivity was obtained by using the modified Maxwell model.

## INTRODUCTION

The thermal diffusivity  $\alpha$  and conductivity  $K$  of polymers are important transport properties both from the theoretical and practical viewpoint. Considerable work has been done during the 1960s, and this has been discussed in several reviews.<sup>1-3</sup> Recently, a flash method has been developed for thermal diffusivity measurements on both isotropic and oriented polymers between 100 and 350 K,<sup>4-6</sup> and in the present work we report the results for nylon 6, poly(ethylene terephthalate) (PET), poly(butylene terephthalate) (PBT), polybutene-1 (PB-1), and poly(4-methylpentene-1) (P4MP1). There has been no previous measurement at all on the last three polymers, even for isotropic samples. The present data are combined with those previously obtained by us and other workers to generate a general pattern for both the temperature and orientation dependence. This dependence will be understood in terms of a two-phase model<sup>7</sup> recently proposed by Choy and Young.

## EXPERIMENTAL

### Sample Preparation

PET (Arnite, AKZO), PBT (Ultradur, BASF), and nylon 6 (Ultramid, BASF) were supplied to us in sheets about 3 mm thick. Sheets of PB-1 and P4MP1 2 mm thick were also prepared from pellets obtained from Scientific Polymer Products Inc. by compression molding above their melting points and then quenching in water at room temperature. Oriented samples were prepared by drawing isotropic sheets of length 4 cm and width 2 cm at a rate of 1 cm/min and at the temperatures shown in Table I.

To investigate the effect of crystallinity, a 0.6-mm-thick sheet of PBT was melted between two thin stainless steel plates and then quenched in water. Another sample of higher crystallinity was prepared by annealing a quenched sheet at 170°C for 1 h.

TABLE I  
 Characteristics of Polymer Samples

Polymer	$\rho_a$ , g/cm <sup>3</sup>	$\rho_c$ , g/cm <sup>3</sup>	Draw temp., °C	Draw ratio	Density $\rho$ , g/cm <sup>3</sup>	Crystal- linity X
Poly(ethylene terephthalate)	1.335 <sup>a</sup>	1.455 <sup>a</sup>	—	1	1.383	0.40
			120	3.2	1.381	
Poly(butylene terephthalate)	1.280 <sup>b</sup>	1.396 <sup>b</sup>	—	1	1.294 <sup>c</sup>	0.12
			—	1	1.319 <sup>d</sup>	0.34
			—	1	1.317 <sup>e</sup>	0.32
			100	3.2	1.314	
Nylon 6	1.10 <sup>f</sup>	1.23 <sup>g</sup>	—	1	1.147	0.36
			100	2.5	1.145	
Polybutene-1	0.871 <sup>h</sup>	0.952 <sup>h</sup>	—	1	0.916	0.55
			70	2.4	0.916	
Poly(4-methylpentene-1)	0.838 <sup>i</sup>	0.828 <sup>i</sup>	—	1	0.834	0.23 <sup>j</sup>
			70	6	0.833	

<sup>a</sup> Reference 8.

<sup>b</sup> Reference 9.

<sup>c</sup> Quenched sample.

<sup>d</sup> Quenched and then annealed for 1 h at 170°C.

<sup>e</sup> As-received sheet.

<sup>f</sup> Reference 10.

<sup>g</sup> Reference 11.

<sup>h</sup> Reference 12.

<sup>i</sup> Reference 13.

<sup>j</sup> Estimated from heat of fusion.

The densities  $\rho$  of all the isotropic samples except P4MP1 were measured by the flotation method, and the volume fraction crystallinities  $X$  were calculated by using the literature values for the densities of the amorphous ( $\rho_a$ ) and crystalline ( $\rho_c$ ) phases and the equation

$$X = \frac{\rho - \rho_a}{\rho_c - \rho_a}$$

The values of  $\rho$ ,  $\rho_a$ ,  $\rho_c$ , and  $X$  are given in Table I. The densities remain roughly unchanged after drawing, so it seems reasonable to assume that  $X$  is the same for both the isotropic and oriented samples. For P4MP1,  $\rho_a$  and  $\rho_c$  are roughly the same at room temperature, so another method has to be used. We have measured the heat of fusion  $H$  of this polymer using a Perkin-Elmer DSC-2 differential scanning calorimeter and have obtained the crystallinity from the relation

$$X = \frac{H}{H_c} \frac{\rho}{\rho_c}$$

where  $H_c = 29$  cal/g is the heat of fusion of the crystalline phase of P4MP1.<sup>14</sup>

For use in actual measurements, the oriented sheets were first cut into rectangular strips of equal length but varying width. They were then glued together on the flat side by intervening layers of epoxy resin so as to form roughly a right circular cylinder, with the draw direction  $\hat{n}$  of the polymer strips either parallel or perpendicular to the cylinder axis for the measurement of thermal diffusivity along or normal to  $\hat{n}$ , respectively.

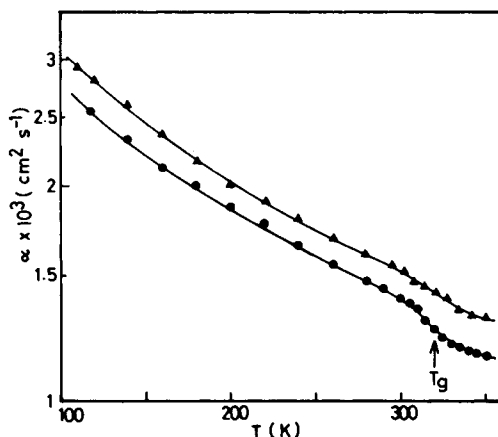


Fig. 1. Temperature dependence of thermal diffusivity of two samples of PBT with different degree of crystallinity  $X$ : (●)  $X = 0.12$ ; (▲)  $X = 0.34$ .  $T_g$  denotes the glass transition.

The diffusivity  $\alpha$  was measured by the flash method, which has already been described in detail previously.<sup>4-6</sup> In essence, a heat pulse was delivered at the front surface of an isolated sample cylinder by the use of a flash lamp, thus generating a transient temperature difference between the front and back surfaces of the sample, which was sensed by thermocouple junctions attached to the surfaces and recorded on a potentiometric recorder. The diffusivity  $\alpha$  can then be deduced from the exponential decay time constant  $t_c$  of the temperature difference and the length  $L$  of the sample through the relation  $\alpha = L^2/\pi^2 t_c$ , and corrections were made for various systematic errors, especially the effect of glue

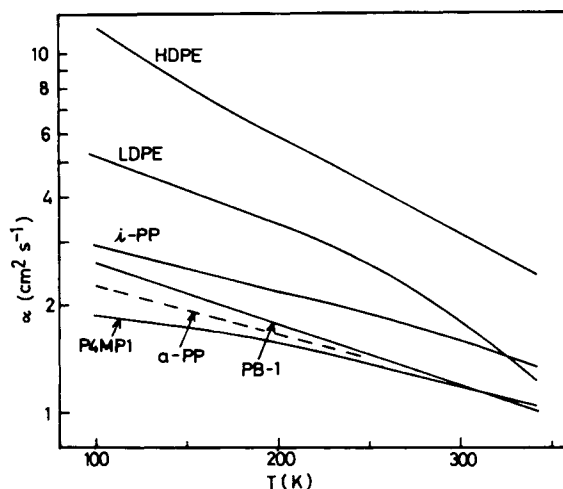


Fig. 2. Temperature dependence of thermal diffusivity of various polyolefins. HDPE and LDPE denote high- and low-density polyethylene, respectively, and *i*-PP and *a*-PP represent isotactic and atactic polypropylene, respectively. Data for HDPE, LDPE and *i*-PP are taken from ref. 6, and data for *a*-PP are taken from ref. 20. Data of PB-1 and P4MP1 are from the present work. The crystallinities of HDPE, LDPE, *i*-PP, *a*-PP, PB-1, and P4MP1 are 0.8, 0.42, 0.6, 0, 0.55, and 0.23, respectively. For the sake of clarity, smooth curves have been drawn to represent discrete data points.

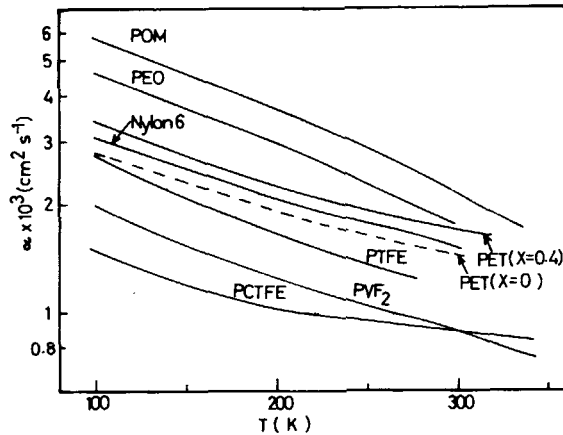


Fig. 3. Temperature dependence of thermal diffusivity of various polymers. The oxide polymers are poly(oxymethylene (POM), poly(ethylene oxide) (PEO) and the fluoropolymers are poly(tetrafluoroethylene) (PTFE), poly(vinylidene fluoride) (PVF<sub>2</sub>), and poly(chlorotrifluoroethylene) (PCTFE). Data for POM, PET, PVF<sub>2</sub>, and PCTFE are taken from refs. 4 and 6; data for PEO and PTFE are taken from refs. 22 and 21, respectively. Data for nylon 6 are from the present work. The crystallinities  $X$  of POM, PEO, nylon 6, PVF<sub>2</sub>, and PCTFE are 0.63, 0.8, 0.36, 0.46, and 0.4, respectively. The crystallinity of the PTFE sample is unknown.

and radiation loss at sample surfaces, which became considerable at high temperature.

The conductivity  $K$  can then be determined through the relation  $K = \rho C \alpha$ , where the specific heat  $C$  at the relevant temperature is usually available in literature,<sup>14-18</sup> while it suffices to use the room-temperature value for density  $\rho$ , as it does not vary much over the entire temperature range. Since the specific heat of PBT is not available, it was measured at a heating rate of 10°C/min on a Perkin-Elmer DSC-2 differential scanning calorimeter by following standard procedure.<sup>19</sup> The accuracy was estimated to be 4%.

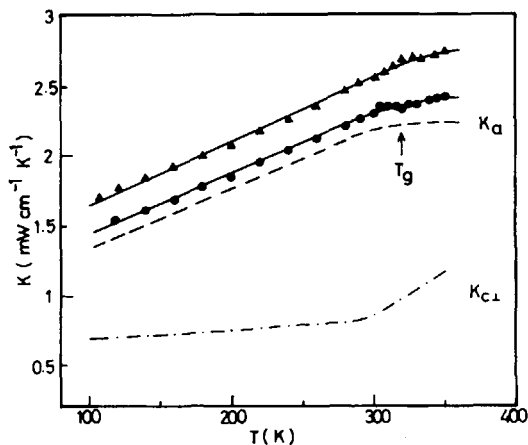


Fig. 4. Temperature dependence of thermal conductivity of two samples of PBT with different degree of crystallinity  $X$ : (●)  $X = 0.12$ ; (▲)  $X = 0.34$ .  $T_g$  denotes the glass transition.  $K_a$  and  $K_{c\perp}$  denote the thermal conductivity of the amorphous regions and the thermal conductivity normal to the chain axis of the crystallites, respectively.  $K_a$  and  $K_{c\perp}$  have been calculated from the data according to eq. (1).

## RESULTS AND DISCUSSION

## Thermal Diffusivity

The thermal diffusivities  $\alpha$  of two samples of PBT with different crystallinity ( $X = 0.12$  and  $0.34$ ) are shown in Figure 1. For the sample with  $X = 0.12$ , an abrupt drop in  $\alpha$  is observed near the glass transition ( $T_g \approx 320$  K), consistent with the behavior of amorphous polymers such as poly(ethylene terephthalate).<sup>4</sup> However, for the sample with higher crystallinity ( $X = 0.34$ ), the transition is more diffused and hence not so noticeable. It is also apparent that  $\alpha$  is weakly dependent on crystallinity  $X$  and increases by only 10–15% as  $X$  increases from 0.12 to 0.34.

The thermal diffusivities of PB-1, P4MP1, nylon 6, and PET are shown in Figures 2 and 3, together with the data for other polymers obtained in previous studies.<sup>4-6,20-22</sup> It is clear from Figures 1–3 that  $\alpha$  decreases with rising temperature as  $T^{-\gamma}$ , with  $0.5 < \gamma < 1$ . The temperature dependence is stronger for those polymers (such as HDPE and POM) that have a higher  $\alpha$  value. As a result,  $\alpha$  of HDPE at 100K is about five times larger than that of P4MP1, but the difference becomes much smaller at 340 K (Fig. 2).

For the series of polyolefins in Figure 2, polyethylene, the polymer with the simplest chemical structure, has the highest  $\alpha$ . Even LDPE, with a crystallinity of only 0.42, has a value much larger than isotactic PP of crystallinity 0.6. Before discussing the effect of crystallinity, it should be noted that the thermal diffusivity is roughly the same for all amorphous polymers,<sup>3</sup> and the data on atactic

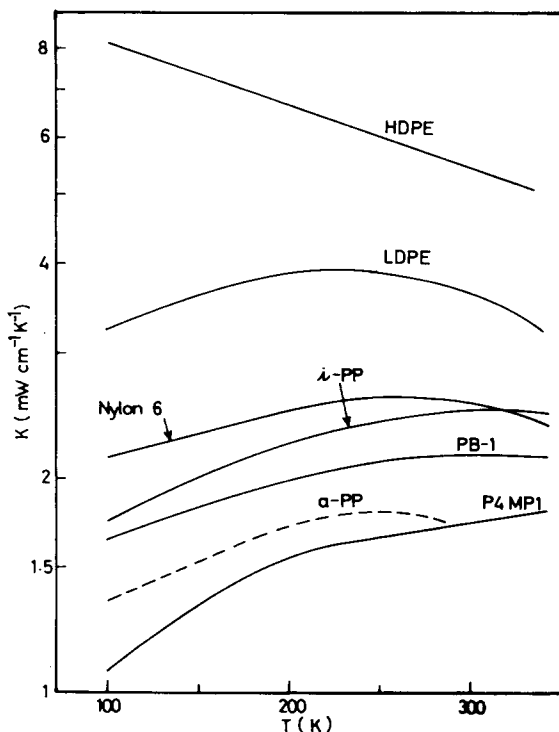


Fig. 5. Temperature dependence of the thermal conductivity of various polymers. Legends are the same as for Fig. 2.

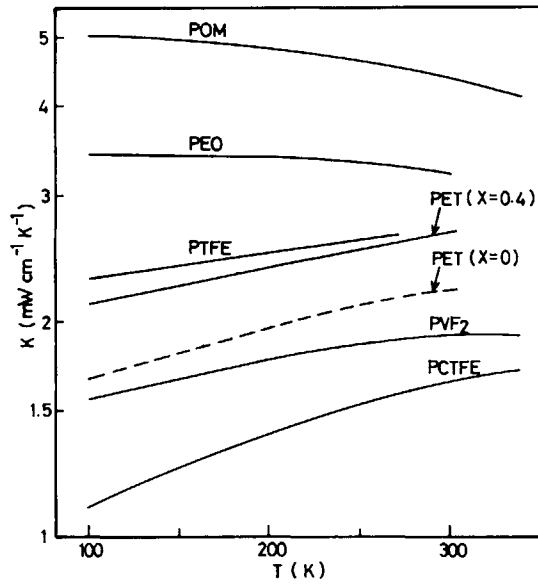


Fig. 6. Temperature dependence of the thermal conductivity of various polymers. Legends are the same as for Fig. 3.

PP and amorphous PET given in Figures 2 and 3 can be taken as typical. Figure 2 also shows that PE exhibits very strong crystallinity dependence, whereas  $\alpha$  for PP increases by only 30% for a crystallinity change from 0 to 0.6. The data for PB-1 ( $X = 0.55$ ) and P4MP1 ( $X = 0.23$ ) are slightly higher and lower, respectively, than the typical values for amorphous polymers; so it is reasonable to assume that, like PP, they also exhibit weak crystallinity dependence.

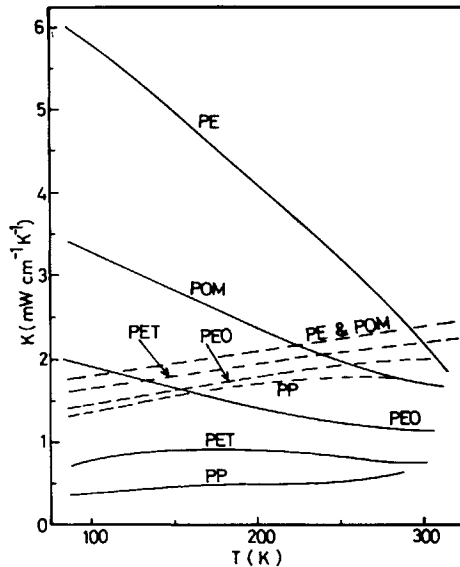


Fig. 7. Temperature dependence of thermal conductivity of the amorphous regions ( $K_a$ ) and the thermal conductivity normal to the chain axis of the crystallites ( $K_{c\perp}$ ). Dashed and full curves denote  $K_a$  and  $K_{c\perp}$ , respectively.

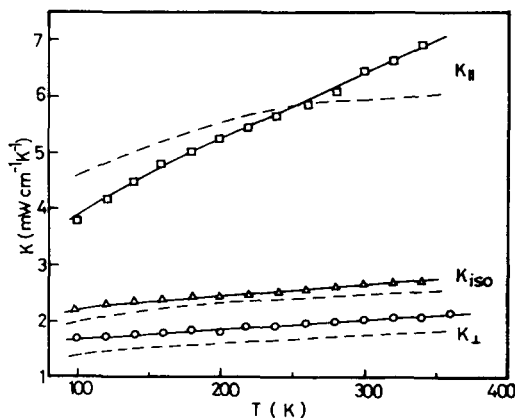


Fig. 8. Temperature dependence of thermal conductivity of oriented PET. Dashed lines represent theoretical predictions according to eqs. (1)–(3) with  $f_c = 0.9$ .

Turning now to Figure 3, we see that the highly crystalline oxide polymers POM ( $X = 0.68$ ) and PEO ( $X = 0.8$ ) have thermal diffusivities roughly the same as LDPE ( $X = 0.42$ ). As a group, the fluoropolymers have very low thermal diffusivity, comparable to that of an amorphous polymer. The values for nylon 6, PET, and PBT are very close to one another and lie between those for the oxide and fluoropolymers.

### Thermal Conductivity

Figure 4 shows the thermal conductivity  $K$  of two samples of PBT with crystallinity 0.12 and 0.34, respectively. For the sample with  $X = 0.12$ ,  $K (= \rho C \alpha)$  exhibits only a change of slope near  $T_g$ , in contrast to the abrupt drop observed for  $\alpha$  (see Fig. 1), which implies that this drop has been compensated by the sudden rise in  $C$ . Similar to  $\alpha$ ,  $K$  is also weakly dependent on crystallinity and increases by only 15% for a 22% rise in crystallinity.

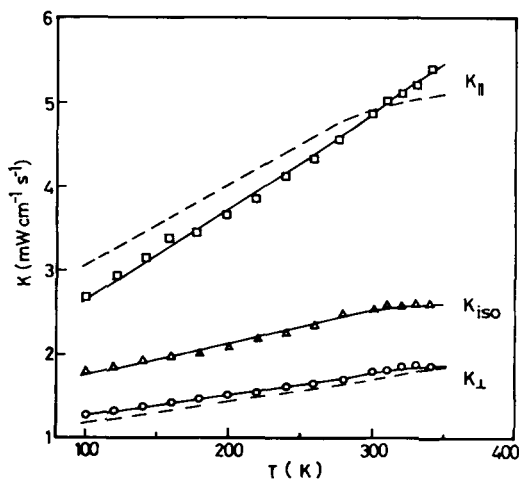


Fig. 9. Temperature dependence of thermal conductivity of oriented PBT. Dashed lines represent theoretical predictions according to eqs. (1)–(3) with  $f_c = 0.9$ .

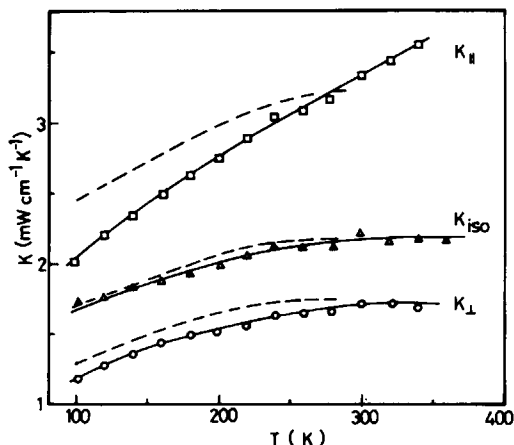


Fig. 10. Temperature dependence of thermal conductivity of oriented PB-1. Dashed lines represent theoretical predictions according to eqs. (1)–(3) with  $f_c = 0.3$ .

The thermal conductivities of the other polymers are shown in Figures 5 and 6. It is seen that the temperature dependence of  $K$  is quite different from that of  $\alpha$  because the specific heat  $C$  also has significant temperature dependence. Thus, the values of  $K$  for different polymers follow roughly the same order as  $\alpha$ , yet  $K$  for most polymers (excepting HDPE, POM, and PEO) has a positive rather than a negative temperature coefficient. This feature can be readily understood in terms of the modified Maxwell model,<sup>7</sup> which assumes that a semicrystalline polymer is made up of anisotropic spherical crystallites imbedded in an isotropic amorphous matrix. The thermal conductivity  $K_{\text{iso}}$  of an isotropic sample is then given by

$$K_{\text{iso}} = K_a \left[ 1 + \frac{3Xk_{\perp}}{2 + (1 - X)k_{\perp}} \right] \quad (1)$$

where  $X$  is the volume fraction crystallinity,  $K_a$  is the thermal conductivity of the amorphous phase and  $k_{\perp} = K_{c\perp}/K_a$ ,  $K_{c\perp}$  being the thermal conductivity

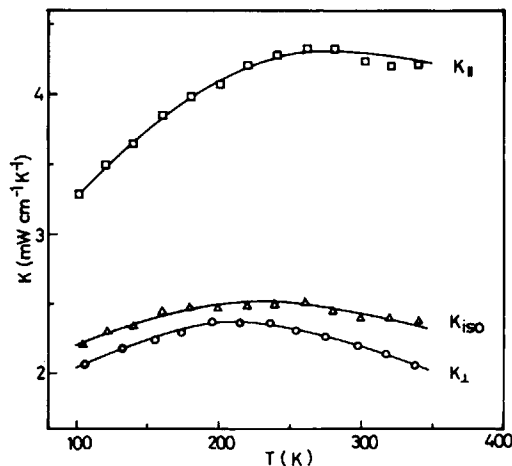


Fig. 11. Temperature dependence of thermal conductivity of oriented nylon 6.



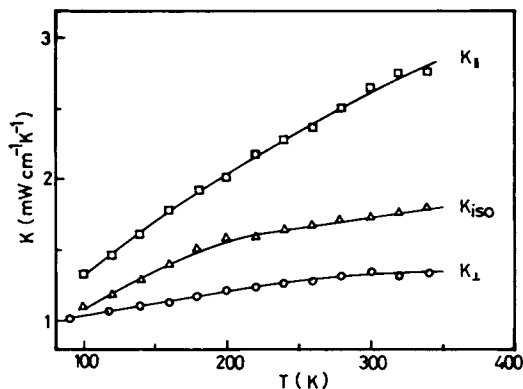


Fig. 12. Temperature dependence of thermal conductivity of oriented P4MP1.

of the crystallites normal to the chain axis. The thermal conductivity along the chain axis of the crystallites  $K_{c\parallel}$  does not appear in eq. (1) as a result of the assumption  $K_{c\parallel} \gg K_a$ ; that is,  $K_{c\parallel}$  is so large that its effect has been saturated.

It is clear from eq. (1) that  $K_a$  and  $K_{c\perp}$  can be calculated from the observed  $K_{iso}$  at two different crystallinities, and this has been done for PBT using the data in Figure 4. However, for five other polymers (PET, PP, PE, POM, and PEO), one of the  $K_{iso}$  used is the value at  $X = 0$  (i.e.,  $K_a$ ) which has been obtained in the following ways. First, direct measurements on atactic PP and amorphous PET (see Figs. 5 and 6) are available in the literature.<sup>4,20</sup> Secondly, for PE, POM, and PEO, the procedure adopted is to extrapolate from the conductivities of the respective melts<sup>22-24</sup> down to lower temperature. This seems reasonable since the amorphous phase may be regarded as a supercooled state of the melt. The results are probably reliable to within 15% because the values so obtained fall within the universal range for all amorphous polymers,<sup>3</sup> i.e.,  $K_a$  varies from  $1.5 \pm 0.3$  mW/cm · K at 100 K to  $2.0 \pm 0.4$  mW/cm · K at 300 K.

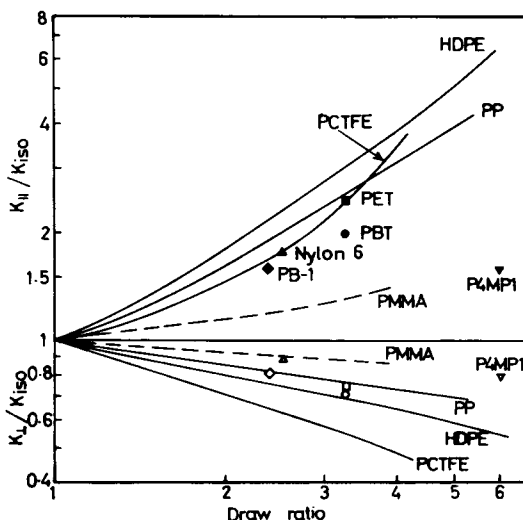


Fig. 13. Draw ratio dependence of thermal conductivity of various oriented polymers. The data for HDPE ( $X = 0.8$ ), PP ( $X = 0.6$ ), and PCTFE ( $X = 0.4$ ) are taken from ref. 6, and the data for PMMA ( $X = 0$ ) are taken from ref. 27.

The intrinsic conductivities  $K_a$  and  $K_{c\perp}$  of PBT and the other five polymers are shown as functions of temperature in Figures 4 and 7, respectively. It is seen that  $K_{c\perp}$  for the group PE, POM, and PEO is higher and decreases with rising temperature, while  $K_{c\perp}$  for PBT, PET, and PP has a rather weak temperature dependence. We have previously attributed<sup>3,7</sup> the roughly  $T^{-1}$  dependence for PE as characteristic of three-phonon Umklapp scattering processes in the perfect crystals. The fact that  $K_{c\perp}$  for PBT, PET, and PP has a weaker temperature dependence and a much lower magnitude indicates that, for these polymers of more complicated structure, phonon scattering by defects is the dominant mechanism contributing to the thermal resistance. For POM and PEO, both these scattering processes seem to be important.

The magnitude of  $K_{c\perp}$  for the remaining polymers i.e., nylon 6, PB-1, P4MP1, and the fluoropolymers, can also be estimated from eq. (1). It is clearly seen from Figures 5 and 6 that the thermal conductivity of these polymers are similar in magnitude and temperature dependence to those of isotactic PP and PET; therefore, the corresponding  $K_{c\perp}$  should also be similar. Thus, for most polymers, defect scattering of phonons should be the dominant mechanism controlling thermal conduction in the crystallites transverse to the chain direction.

The thermal conductivity of oriented polymers along ( $K_{\parallel}$ ) and normal ( $K_{\perp}$ ) to the draw direction is shown in Figures 8–12 together with the data for the isotropic sample ( $K_{\text{iso}}$ ). It is seen that  $K_{\parallel}$  is much higher than  $K_{\perp}$ , with  $K_{\text{iso}}$  lying in between. The anisotropy  $K_{\parallel}/K_{\perp}$  is largest for PET ( $\lambda = 3.2$ ), with a room-temperature value of 3.5, while the anisotropy for PB-1 ( $\lambda = 2.4$ ), P4MP1 ( $\lambda = 6$ ), and nylon 6 ( $\lambda = 2.5$ ) is only about 2.

The effect of orientation can also be analyzed using the modified Maxwell model<sup>7</sup> which gives

$$\frac{K_{\parallel} - K_a}{K_{\parallel} + 2K_a} = \frac{X(k_{\perp} + 2f_c)}{k_{\perp} + 2} \quad (2)$$

$$\frac{K_{\perp} - K_a}{k_{\perp} + 2K_a} = \frac{X(k_{\perp} - f_c)}{k_{\perp} + 2} \quad (3)$$

where  $f_c$  is the crystalline orientation function of the oriented sample. The values of the parameters  $K_a$ ,  $K_{c\perp}$ , and  $f_c$  are therefore required for the detailed analysis of the thermal conductivity data. For PET and PBT,  $K_a$  and  $K_{c\perp}$  are taken from Figures 7 and 4, respectively, while  $f_c$  of the oriented PET sample ( $\lambda = 3.2$ ) is taken from the literature.<sup>25</sup> Because of lack of data, the same  $f_c$  value (0.9) is assumed for the oriented PBT sample ( $\lambda = 3.2$ ) since its chemical structure is similar. For PB-1, the  $f_c$  value (= 0.3) is available,<sup>26</sup> but we have to assume that the  $K_a$  and  $K_{c\perp}$  values for PP are also appropriate for this polymer. For the two remaining polymers, P4MP1 and nylon 6, no detailed analysis has been attempted because of lack of relevant data.

In Figures 8–10, we see that the theoretical predictions (dashed curves) for PET, PBT, and PB-1 agree with the experimental data to within 20%. This seems reasonable in view of the crude assumptions involved in obtaining the relevant parameters as previously discussed.

Finally, the data for the oriented samples are summarized in  $K_{\parallel}/K_{\text{iso}}$  and  $K_{\perp}/K_{\text{iso}}$  plots in Figure 13. For comparison, data for four polymers with increasing degree of crystallinity—poly(methyl methacrylate) (PMMA,  $X = 0$ ),

poly(chlorotrifluoroethylene) (PCTFE,  $X = 0.4$ ), PP ( $X = 0.6$ ), and HDPE ( $X = 0.8$ )—are also shown. We see that  $K_{\parallel}/K_{\text{iso}}$  increases quite rapidly with draw ratio  $\lambda$ , and the rate of increase is larger the higher the crystallinity; whereas  $K_{\perp}/K_{\text{iso}}$  shows only a slight decrease. Our present data on PET ( $X = 0.4$ ), PB-1 ( $X = 0.55$ ), nylon 6 (0.36), and PBT ( $X = 0.34$ ) roughly follow these trends, and the  $K_{\parallel}/K_{\text{iso}}$  data lie close to the curve for PCTFE ( $X = 0.4$ ). P4MP1 seems to be the only exception, since its  $K_{\parallel}/K_{\text{iso}}$  value is similar to that of PMMA (an amorphous polymer), which probably results from the low crystallinity ( $X = 0.23$ ) and the low degree of crystalline orientation in the sample.

The authors are grateful to BASF for supplying the sheets of poly(butylene terephthalate) and nylon 6.

### References

1. D. E. Kline and D. Hansen, in *Thermal Characterization Techniques*, P. E. Slade and L. J. Jenkins, Eds., Marcel Dekker, New York, 1970, p. 247.
2. W. Knappe, *Adv. Polym. Sci.*, **7**, 477 (1971).
3. C. L. Choy, *Polymer*, **18**, 984 (1977).
4. F. C. Chen, Y. M. Poon, and C. L. Choy, *Polymer*, **18**, 129 (1977).
5. C. L. Choy, W. H. Luk, and F. C. Chen, *Polymer*, **19**, 155 (1978).
6. C. L. Choy, F. C. Chen, and W. H. Luk, *J. Polym. Sci. Phys. Ed.*, **18**, 1187 (1980).
7. C. L. Choy and K. Young, *Polymer*, **18**, 769 (1977).
8. R. P. Daubeny, C. W. Bunn, and C. J. Brown, *Proc. Roy. Soc. (London)*, **A226**, 531 (1954).
9. A. Misra and R. S. Stein, *Bull. Am. Phys. Soc. Ser. II*, **20**, 341 (1975).
10. A. Ziabicki, *Kolloid Z. Z. Polym.*, **167**, 132 (1959).
11. D. R. Holmes, C. W. Bunn, and D. J. Smith, *J. Polym. Sci.*, **17**, 159 (1955).
12. H. Wilski and T. Grewer, *J. Polym. Sci. (C)*, **6**, 33 (1964).
13. J. H. Griffith and B. G. Ranby, *J. Polym. Sci.*, **44**, 369 (1960).
14. F. E. Karasz, H. E. Bair, and J. M. O'Reilly, *Polymer*, **8**, 547 (1967).
15. E. Yu Roinishvili, N. N. Tavkhelidze, and V. B. Akopyan, *Vysokomol. Soedin. Ser. B*, **9**, 254 (1967).
16. F. S. Dainton, D. M. Evans, F. E. Hoare, and T. P. Melia, *Polymer*, **3**, 286 (1962).
17. V. P. Kolesov, I. E. Paukov, and S. M. Skuratov, *Zh. Fiz. Khim.*, **36**, 770 (1962).
18. B. Wunderlich and H. Baur, *Adv. Polym. Sci.*, **7**, 151 (1970).
19. *Instruction Manual for DSC-2 Differential Scanning Calorimeter*, Perkin-Elmer Corporation, Norwalk, Conn.,
20. K. Eiermann, *Kolloid Z. Z. Polym.*, **201**, 3 (1965).
21. K. Eiermann and K. H. Hellwege, *J. Polym. Sci.*, **57**, 99 (1962).
22. K. H. Hellwege, R. Hoffmann, and W. Knappe, *Kolloid Z. Z. Polym.*, **226**, 109 (1968).
23. W. Knappe and P. Lohe, *Kolloid Z. Z. Polym.*, **189**, 114 (1963).
24. R. B. Shoulberg, *J. Appl. Polym. Sci.*, **7**, 1597 (1963).
25. J. H. Dumbleton, *J. Polym. Sci. (A-2)*, **7**, 667 (1969).
26. S. Hoshino, J. Powers, D. G. Legrand, H. Kawai, and R. S. Stein, *J. Polym. Sci.*, **58**, 185 (1962).
27. J. Hennig and W. Knappe, *J. Polym. Sci. (C)*, **6**, 167 (1964).

Received August 20, 1980

Accepted December 24, 1980